Molecular dynamics simulation of the energetic reaction between Ni and Al nanoparticles

Brian J. Henz,[1] Takumi Hawa,[3] and Michael Zachariah[2,3,a)]
[1]*U.S. Army Research Laboratory, Aberdeen Proving Ground, Maryland, 21005, USA*
[2]*National Institute of Standards and Technology, Gaithersburg, Maryland, 20899, USA*
[3]*Department of Mechanical Engineering and Department of Chemistry and Biochemistry, University of Maryland, College Park, Maryland, 20742, USA*

Molecular dynamics simulations are used to simulate the energetic reaction of Ni and Al particles at the nanometer scale. The effect of particle size on reaction time and temperature for separate nanoparticles has been considered as a model system for a powder metallurgy system. Coated nanoparticles in the form of Ni-coated Al nanoparticles and Al-coated Ni nanoparticles are also analyzed as a model for nanoparticles embedded within a matrix. The differences in melting temperature and phase change behavior, e.g., the volumetric expansion of Al between Al and Ni, are expected to produce differing results for the coated nanoparticle systems. For instance, the volumetric expansion of Al upon melting is expected to produce large tensile stresses and possibly rupture in the Ni shell for Ni-coated Al. Simulation results show that the sintering time for separate and coated nanoparticles is nearly linearly dependent on the number of atoms or volume of the sintering nanoparticles. We have also found that nanoparticle size and surface energy are important factors in determining the adiabatic reaction temperature for both systems at nanoparticle sizes of less than 10 nm in diameter. © *2009 American Institute of Physics*. [DOI: 10.1063/1.3073988]

I. INTRODUCTION

Nanoparticles have interesting physical properties that often vary from the bulk material. Some of these properties, including increased reactivity,[1] are due to the high surface area to volume ratio of nanoparticles. With that in mind nanoparticles may provide enhanced energy release rates for explosive and propellant reactions.[2]

There is a considerable interest in the self-propagating high-temperature synthesis (SHS) reactions of intermetallic compounds because of the associated energy release that takes place[3] during the alloying reaction. In addition to the energetic reaction observed in these materials it is possible to produce structural materials that contain this energy release property. Once ignited, the SHS reaction releases a large amount of energy in a short period of time. One significant difference between SHS and typical combustion processes is that the reactants and products are confined to the condensed state.[4] The SHS process has many potential applications where heat generation is required and oxygen is not available or gaseous products are not desirable. These include alloy formation, net-shape processing, propellants, and as initiators. One of the compounds formed from the SHS reaction, and studied here, is NiAl or nickel aluminide. NiAl is an important alloy because of its desirable high temperature strength and oxidation resistance[5] and the high energy of formation.[6] Recently Weihs and co-workers[7] also used the NiAl nanolaminate systems in applications of reactive welding.

Not surprisingly since the reaction involves solid starting materials, particle size has a significant effect on the properties of the reaction product and the SHS reaction itself.[8] The simulation and analysis of nanoparticle coalescence without the SHS reaction for like materials are extensive[9–14] and involve surface passivation,[10] size differences,[9,11] and phase change[9] considerations. The analysis here includes all of the previously listed concerns with an additional energy release term from the heat of formation.

The focus of this paper is to use atomistic simulation to model the reactive behavior of Ni–Al nanoparticles in various configurations. Fortunately, there have been numerous efforts to determine the accurate empirical potentials for simulating the Ni–Al material system.[15] Prior simulations using these potentials have investigated the diffusion of Ni and Al atoms,[15] point-defect concentrations in NiAl,[16] and plasticity[17] in addition to many other mechanical and chemical properties. These efforts have primarily focused on bulk materials rather than nanoparticle systems,[18] even though there are many manufacturing processes that produce nanometer sized powders for SHS reactions.[19] For this simulation effort we have chosen a set of embedded atom method (EAM) parameters that reproduce reasonably well the properties of Ni, Al, and NiAl in the temperature range of interest.

II. SIMULATION APPROACH

In this work we employ classical molecular dynamics (MD) with an EAM interatomic potential to study the SHS reaction. The EAM is used because of its accuracy and capability to scale up to material systems with over 10^6 atoms.

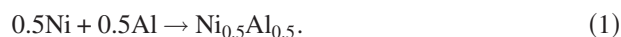a)Author to whom correspondence should be addressed. Electronic mail: mrz@umd.edu.

The MD simulations are compared with thermodynamic analyses in order to provide validation of the simulation results and assess the expected energy release.

The MD simulation was conducted using the LAMMPS software package.[20] For the Ni–Al interactions the Finnis–Sinclair EAM potential[21] with parameters from Angelo et al.[22] was used. The Finnis–Sinclair EAM potential allows for nonsymmetric embedding potential terms, potentially providing improved accuracy for metallic alloys.[23] In addition to the parameters for NiAl from Angelo et al.[22] other authors have also developed parameters for the Ni–Al system[16] that may also be described by using the Finnis–Sinclair EAM.

Three primary nanoparticle sizes considered in this work from smallest to largest are nanoparticles with 1289, 5635, and 36 523 atoms each, which correspond approximately to 3, 5, and 10 nm, respectively. The range of sizes was chosen because it represents nanoparticles that may be produced in the laboratory and which offers reasonable computational time to conduct parametric studies. For the largest system studied, the 10 nm diameter nanoparticle energetic reaction simulation requires ~2 days and 64 processor cores to complete a few nanoseconds of simulated time on 3.0 GHZ INTEL WOODCREST processors.

III. THERMODYNAMIC ANALYSIS OF SEPARATE NANOPARTICLES

The separate nanoparticle system is used as a model for powder metallurgy systems where Ni and Al particles are compressed into a structural component. In addition to mechanical properties, the structural component will contain stored energy for future release through a SHS reaction. A thermodynamic analysis of the SHS reaction for the separate Ni and Al nanoparticle systems is used here to determine the expected trends and data points for simulation validation. In the thermodynamic analysis we are interested in determining the system parameters of the Ni–Al nanoparticle system that contribute to the combustion temperature and reaction time. Here we have assumed an adiabatic process so that energy released to the surroundings can be ignored. This is a good approximation since the reaction occurs on relatively short time scales and the nanoparticles are expected to be included in a much larger system where the overall surface to volume ratio is small, limiting convective and radiative heat loss. The validity of this assumption is explored in Secs. V and VI. The SHS reaction of an equimolar Ni and Al mixture is written as

$$0.5Ni + 0.5Al \rightarrow Ni_{0.5}Al_{0.5}. \tag{1}$$

In order to compute the adiabatic temperature for the synthesis reaction the enthalpy of the products and reactants must be equal,

$$H_{prod}(T_{ad}) = H_{reac}(T_0). \tag{2}$$

Assuming that the reaction begins with the reactants at 600 K, above the simulated melting temperature of the Al nanoparticles, the enthalpy of the reactants is computed as

TABLE I. Change in surface energy vs nanoparticle size.

Nanoparticle radius (nm)	ΔE_{surf} (kJ/mol)
3	−18.35
5	−11.41
10	−6.17

$$H_{reac} = (0.5)(H_{Al,fusion}) + (0.5)(H_{Al,600\ K} + H_{Ni,600\ K})$$
$$= 11.85\ \text{kJ/mol.} \tag{3}$$

This enthalpy result includes the enthalpy of solid Ni and liquid Al.[6] The Al nanoparticle is assumed to be liquid because for small nanoparticles the melting temperature is known to be appreciably below the bulk melting temperature.[24] Additionally, for the EAM potential used here[22] the aluminum is liquid for these nanoparticle sizes at 600 K. The choice of initial temperature will have a nearly linear effect on the adiabatic temperature as long as the temperature is between the melting temperature of the Al and Ni nanoparticles. This linear effect has been observed in experiments[25] and is a reasonable assumption so long as the heat capacities of the solid phases of Ni and NiAl are relatively insensitive to temperature in the ranges studied.

For the products of the SHS process the enthalpy calculation must take into account the contributions from the melting of the nickel and the NiAl nanoparticle, enthalpy of formation for the NiAl alloy, and changes in surface energy. The first of these, the enthalpies of melting for Ni and NiAl, is experimentally determined to be 17.2 and 31.4 kJ/mol, respectively. The enthalpy of mixing for Ni and Al has garnered close scrutiny in the experimental community with a wide range of reported values. The enthalpy of formation that is used here is approximately in the middle of the reported values at about −65 kJ/mol.[6,26,27]

The last contribution to the enthalpy of the products results from the change in surface energy due to the reduced total surface area of the combined nanoparticle.[28] The contribution to the change in system energy from the change in surface area is given as

$$\Delta E_{surf} = \sigma_{NiAl}a_{NiAl} - (\sigma_{Ni}a_{Ni} + \sigma_{Al}a_{Al}). \tag{4}$$

In Eq. (4), a_{NiAl}, a_{Ni}, and a_{Al} are the surface area of the NiAl, Ni, and Al nanoparticles, respectively. For the 3, 5, and 10 nm Al nanoparticles the reactant surface area is computed from the Gibbs surface[29] as 36.32, 98.17, and 343.7 nm^2, respectively. For the associated Ni nanoparticles the surface area is 27.15, 73.59, and 257.87 nm^2, respectively. The surface energy is ~1115 mJ/m^2 for Al and 2573 mJ/m^2 for Ni at 600 K.[30] The surface area of the sintered NiAl nanoparticles is 50.77, 137.18, and 480.25 nm^2 for the 3, 5, and 10 nm nanoparticle cases, respectively. In the experimental analysis of the free surface energy of NiAl near its melting point, the free surface energy has been reported as 1400 mJ/m^2.[31] The approximate change in energy versus nanoparticle size is tabulated in Table I. In Table I the trend is for a lower surface energy contribution to the reaction as the nanoparticle size increases. Intuitively, one may expect

TABLE II. Computed adiabatic temperature vs nanoparticle radius including contact of flat surfaces or infinitely sized spheres.

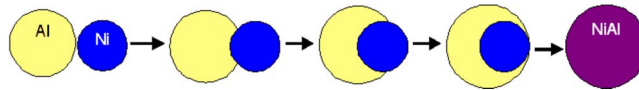| Nanoparticle radius (nm)	T_{ad} (K)
3	2115
5	1920
10	1772
∞	1599

FIG. 1. (Color online) Illustration of sintering process showing the liquid Al nanoparticle first coating the solid Ni nanoparticle and then complete alloying after the Ni nanoparticle has melted.

this because the surface area to volume ratio is also decreasing with increasing particle size and therefore has less influence on the sintering process. With the enthalpy of formation for NiAl around −65 kJ/mol, the surface energy contribution to the change in enthalpy for coalescence of 10 nm diameter nanoparticles is less than 10% of the total enthalpy change. This means that even at relatively small nanoparticle sizes, e.g., 10 nm, the effect of nanoparticle size on energy release is minimal.

With the preceding discussion it is possible to take into account many of the sources of enthalpy change in the reaction products including phase and surface area changes. The enthalpy of the products is now estimated as

$$H_{prod} = H_{form,NiAl} + \Delta H_{surf} + \int_{298\ K}^{T_{ad}} C_{p,NiAl}(T)dT$$

$$+ H_{melt,Ni}. \tag{5}$$

The heat capacity of solid and liquid NiAl is given by Kubaschewski.[32] For the 3 nm case, assuming the NiAl nanoparticle melting temperature to be about 1350 K or the melting point of a similarly sized Ni nanoparticle, it is possible to compute the adiabatic reaction temperature (Table II). Notice in Table II that if no surface energy contribution is considered, i.e., infinitely large spheres, the final adiabatic temperature is computed to be 1599 K. In the simulation section we will observe that these results are reasonable and accurately predict the simulated increase in temperature attributable to the contribution from the surface energy.

IV. THE COALESCENCE PROCESSES

For Ni and Al nanoparticles the SHS reaction consists of two processes, namely, coalescence and alloying. In this work we have considered the coalescence of a two nanoparticle system with an Al and a Ni nanoparticle with an atomic ratio of unity. A complete SHS reaction of this system will result in a single NiAl nanoparticle. The MD simulations used to work model adiabatic conditions with a constant number of atoms and total system energy. The purpose of these simulations is to analyze the effect of nanoparticle size on sintering time, adiabatic combustion temperature, and to visualize the process. The assumed process is illustrated in Fig. 1. In Fig. 1 the nanoparticles are initially in contact at a point (a) and the Al nanoparticle is larger than the Ni nanoparticle because of the longer Al–Al bond length. The simulations are initialized at 600 K so that the Al nanoparticle is liquid and the Ni nanoparticle is solid. In Fig. 1 the sintering process proceeds with the liquid Al nanoparticle initially

coating the solid Ni nanoparticle while forming some Ni–Al bonds on the surface [(b)–(d)]. Next, the alloying process proceeds with the Ni nanoparticle being heated above its melting point and becoming liquid so that mixing may occur (e). The formation of Ni–Al bonds beyond the interfacial surface requires diffusion of Al into the Ni nanoparticle or Ni into the liquid Al. Either of these processes is possible but since diffusion is a relatively slow process in solid materials it is expected that the Ni nanoparticle must melt before the coalescence process proceeds appreciably.

The nanoparticle sintering process is driven by two sources of energy as previously discussed. The first of these is a decrease in surface area that lowers the total surface energy of the system. This energy release mechanism is also observed in the sintering of homogeneous material systems such as silicon nanoparticles.[28,33] The second source of energy is from the reactive synthesis that occurs initially at the interface between the nanoparticles and later throughout the entire system. The energy release from the surface sintering is proportional to the surface area of the Ni nanoparticle that is coated by Al and in the whole system to the total number of Ni and Al atoms. Additionally, with the temperature increase there is a decrease in the viscosity of the liquid aluminum that will affect the predicted coalescence time.

The coalescence of nanoparticles in the liquid and solid phases has been examined extensively.[9–11] These studies are primarily concerned with the coalescence of two liquid or two solid nanoparticles. The analysis of the Ni–Al system requires considering the coalescence of a liquid Al nanoparticle and a solid Ni nanoparticle. Lewis et al.[9] considered the coalescence of a liquid and a solid gold nanoparticle. This is similar to the situation here except that the material system considered was homogeneous.

In Ref. 9, the authors were able to simulate two phases occurring simultaneously for a single material by choosing the size of each nanoparticle such that at a specific temperature the phase of the nanoparticles is different. Lewis found that coalescence proceeded in two stages. First, the contact area was maximized, and second, "sphericization" took place driven by surface diffusion. The first stage is much faster than the second and is very similar to the process observed here where the Al nanoparticle maximizes the contact area and partially coats the Ni nanoparticle. In this case there is an added driving force in addition to the surface energy, specifically the energy release in forming of Ni–Al bonds as compared to the Al–Al and Ni–Ni bonds. During the second stage the atoms in the two nanoparticles diffuse and rearrange until the system becomes a single spherical nanoparticle. This stage is driven strongly by the formation of Ni–Al bonds and is expected to occur on a much shorter time scale
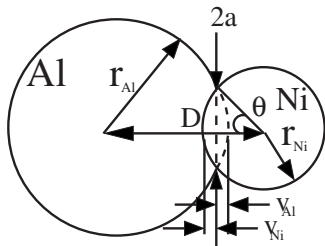
FIG. 2. Illustration of parameters used in analytical model of reactive coalescence of Ni and Al nanoparticles.

than for two nanoparticles of the same material. The analytical model and MD simulation results shown in Secs. V and VI will explore this assumption.

V. PHENOMENOLOGICAL MODEL OF NANOPARTICLE REACTIVE SINTERING

To gain further insight we have developed a phenomenological model for the reactive sintering of Ni and Al nanoparticles. The model includes energy release from surface energy, bond formation, and viscous dissipation through deformation. Frenkel[34] developed a model for the coalescence of two homogeneous nanoparticles; however his model did not account for any phase change, kinetic sintering, or heterogeneous materials. Here we extended Frenkel's model that considers the coalescence of two liquid drops to consider the coalescence of a liquid and a solid drop with reactive synthesis.

The analytical model is initialized with the Al and Ni nanoparticles in contact at a point. The distance from nanoparticle center to center is equal to the sum of the respective radii, denoted as D in Fig. 2. The sintering process initially proceeds by the liquid Al nanoparticle coating the solid Ni nanoparticle, as illustrated in Fig. 1. During this phase of the sintering process, two sources of energy release are occurring. The first of these is related to the decrease in surface area and proportional to the respective surface tension values. The second source of energy release is from the formation of Ni–Al bonds at the interfacial region. Figure 2 is an illustration of the geometric parameters used to model the coalescence time.

In Fig. 2, 2a is the diameter of a circle circumscribed by the contact circumference of the two nanoparticles. v_{Al} and v_{Ni} are the distances from the Al and Ni nanoparticle surfaces to the surface of the contact circle, respectively. θ is the contact angle as measured from the center of the Ni nanoparticle and ranges from 0 to π radians. In order to model the change in energy of the coalescing nanoparticle system, three energy change mechanisms must be considered. These mechanisms are energy release due to change in surface area, energy release due to energetic reactions at the interface, and energy loss due to viscous dissipation. The rate of energy change due to all three must balance at all times.

The first energy term considered, namely, the surface energy of the nanoparticle system, is simply the surface tension times the total exposed surface area. This energy term is written as a sum of the Al and Ni nanoparticle contributions.
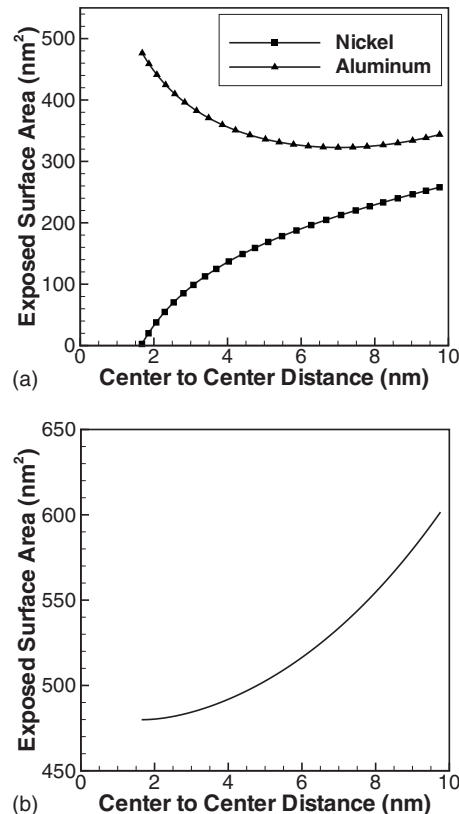

FIG. 3. (a) Plot of exposed Ni and Al nanoparticle surface areas as a function of distance between nanoparticle centers. (b) Plot of total exposed surface area as a function of distance between nanoparticle centers. These results assume a Ni nanoparticle of radius 4.53 nm and an Al nanoparticle of 5.23 nm. Notice that the total exposed surface area is monotonically decreasing, indicating that the surface energy is also decreasing monotonically.

$$E_{\text{surf}} = \sigma_{\text{Ni}}^{s} S_{\text{Ni,exposed}} + \sigma_{\text{Al}}^{l} S_{\text{Al,exposed}}. \tag{6}$$

The exposed area of the Ni nanoparticle can be written as

$$S_{\text{Ni,exposed}} = S_{\text{Ni}} - 2\pi r_{\text{Ni}} v_{\text{Ni}} = 4\pi r_{\text{Ni}}^{2} - 2\pi r_{\text{Ni}} v_{\text{Ni}}, \tag{7}$$

where

$$v_{\text{Ni}} = r_{\text{Ni}}[1 - \cos(\theta)]. \tag{8}$$

Initially during the sintering process the Ni nanoparticle is assumed to remain in the solid phase, thus maintaining a constant radius. This assumption is reasonable because of the higher melting temperature of the Ni nanoparticle.

The exposed surface area of the Al nanoparticle is written as

$$S_{\text{Al,exposed}} = S_{\text{Al}} - 2\pi r_{\text{Al}} v_{\text{Al}} = 4\pi r_{\text{Al}}^{2} - 2\pi r_{\text{Al}} v_{\text{Al}}, \tag{9}$$

where

$$v_{\text{Al}} = r_{\text{Al}} - \sqrt{r_{\text{Al}}^{2} - a^{2}}, \tag{10a}$$

$$a = \sqrt{v_{\text{Ni}}(2r_{\text{Ni}} - v_{\text{Ni}})}. \tag{10b}$$

The radius of the Al nanoparticle is computed numerically by using conservation of volume for the Al nanoparticle. The exposed surface area of each nanoparticle versus the center-to-center distance is plotted in Fig. 3(a). Notice that although the surface area of the Al nanoparticle increases during most of the coalescence process the combined total surface area of
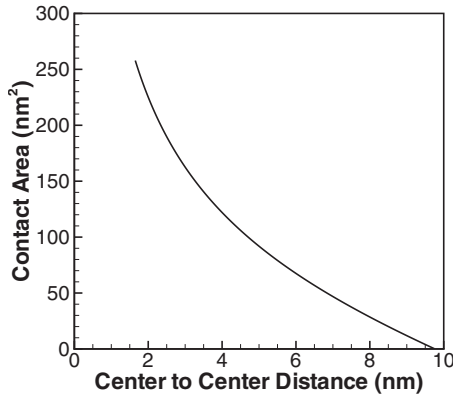
FIG. 4. Contact or interface area as a function of center-to-center distance. The contact area is increasing as the nanoparticles move closer together (right to left on x-axis).
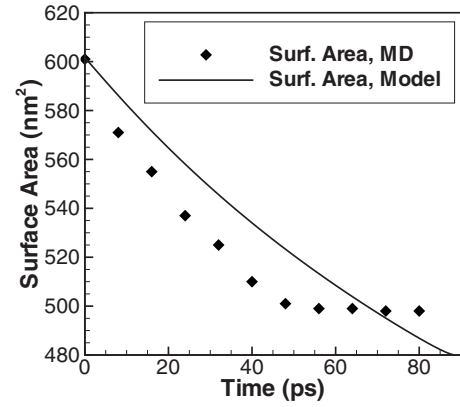

FIG. 5. Total system surface area vs time from mathematical model and MD simulations for the sintering of 10 nm diameter nanoparticles, where the final surface area of the NiAl nanoparticle is ~480 nm².

the Ni and Al nanoparticles decreases monotonically throughout the entire coalescence process. In Fig. 3 the center-to-center distance never reaches zero because the coalescence is considered complete once the Ni nanoparticle is completely enveloped by the Al nanoparticle.

The second source of energy release, namely, the reactive synthesis term, is considered by assuming a constant surface density of the Ni nanoparticle and the transient contact area of the Ni–Al interface,

$$E_{\text{reactive}} = \rho_{\text{Ni,surface}} a_{\text{interface}} V_{\text{bond energy}}. \qquad (11)$$

The surface density term $\rho_{\text{Ni,surface}}$ is proportional to the number of Ni–Al bonds at the contact interface. The surface density and bond energy terms $V_{\text{bond energy}}$ can be combined into a single constant that defines the energy release per unit area of interface,

$$\beta_{\text{density}} = \rho_{\text{Ni,surface}} V_{\text{bond energy}}. \qquad (12)$$

The interfacial contact area is a function of the distance between nanoparticle centers [Fig. 4]. The interfacial area increases monotonically up until the Ni nanoparticle surface is completely covered. This result is expected since the reactive energy term is negative, or releases energy during the entire process, in addition to the minimization of surface energy that is driven by the surface tension of Ni and Al. The interfacial area is written as

$$a_{\text{interface}} = 2\pi v_{\text{Ni}} r_{\text{Ni}}, \qquad (13)$$

where v_{Ni} is a function of θ as given in Eq. (8).

The third energy term represents the viscous dissipation due to deformation of the Al nanoparticle. This viscous dissipation is a function of the viscosity in the liquid Al nanoparticle and the rate of deformation. The extent of the viscous flow can be specified by the decrease in distance between the center of each drop and the surface of contact with the Ni nanoparticle. A velocity gradient γ can be defined as $[(d/dt)D]/r_{\text{Al}}$. The energy dissipated in the whole body per unit time is therefore approximately

$$\frac{dE_{\text{viscous}}}{dt} = 2\eta \int_0^{r_{\text{Al,0}}} \gamma^2 (4\pi r^2) dr = \frac{8}{3}\pi r_{\text{Al,0}}^3 \eta \left(\frac{dD}{dt}\right)^2, \qquad (14)$$

where η is the viscosity of liquid aluminum and $r_{\text{Al,0}}$ is the initial radius of the Al nanoparticle.

By conservation of energy the rate of coalescence can now be computed,

$$\frac{dE_{\text{viscous}}}{dt} = \frac{dE_{\text{surf}}}{dt} + \frac{dE_{\text{reactive}}}{dt}, \qquad (15a)$$

$$\frac{8}{3}\pi r_{\text{Al,0}}^3 \eta \left(\frac{dD}{dt}\right)^2 = \frac{d}{dt}[\sigma_{\text{Ni}}^s S_{\text{Ni,exposed}} + \sigma_{\text{Al}}^J S_{\text{Al,exposed}}]$$

$$+ \frac{d}{dt}[2\beta\pi v_{\text{Ni}} r_{\text{Ni}}]. \qquad (15b)$$

After writing Eq. (15b) in terms of $d\theta/dt$ and simplifying the right and left hand sides we find that Eq. (15b) is only linearly dependent on $d\theta/dt$. Even with this simplification, Eq. (15b) is most easily solved numerically using an iterative solver. In order to solve Eq. (15b) we need some physical properties of Al, Ni, and NiAl. The dynamic viscosity of bulk molten Al at the melting temperature is about $\eta = 1.3 \times 10^{-3}$ Pa s.[35] Based on the comparison of the configurational energy in MD simulations of separate nanoparticles and Al-coated Ni nanoparticles the energy release per unit area β_{density} is estimated to be 20.7 eV/nm². This number is computed by subtracting the system energy of an Al-coated Ni nanoparticle system from the energy of a system with separate nanoparticles and dividing by the interfacial surface area. This method results in the net change in energy during coating of the Ni surface with Al since some Al–Al bonds are lost during the coating process while some Ni–Al bonds are formed at the interface. By numerically solving Eq. (15b) we are able to compute the contact angle θ as a function of time and relate this to total exposed surface area of the coalescing nanoparticles. This result is presented in Fig. 5 along with the comparison to the MD simulation results.

Although qualitatively the results in Fig. 5 show similar trends the absolute rate of coalescence is slightly under predicted by the model. This difference can be attributed to the obvious simplicity of the model and more specifically to the
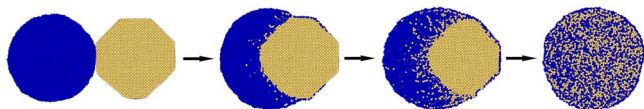
FIG. 6. (Color online) Cross sectional view from MD simulations of Ni/Al nanoparticle sintering process showing the start of the second stage of coalescence where diffusion is the driving force as opposed to contact area maximization. Aluminum atoms are blue and nickel atoms are red.

difficulty in obtaining accurate material parameters. For instance, it is difficult to compare the viscosity of a nanoparticle to the bulk material,[12] and since the coalescence time is linearly dependent on the viscosity a change in viscosity is directly proportional to a change in modeled coalescence time. Additionally, the energy release per unit area term assumes that the net change in energy due to the addition of Ni–Al bonds at the interface is a constant value. This is likely not completely accurate since fewer Al bonds must be broken to form new Ni–Al bonds during the initial contact of the nanoparticles. However, the deviation in this energy release term is likely to be minimal. The deviation of the model time from the simulation results at about 50 ps is due to the switch from stage 1 to stage 2 in the kinetic coalescence process, as described by Lewis *et al.*[9] As described by Lewis, during stage 2, surface diffusion is the predominant factor in continued coalescence and is a much slower process than contact area maximization. The actual simulation results, as compared with the illustration in Fig. 1, of the observed coalescence process are given in Fig. 6.

In Fig. 6 each of the steps in the coalescence process is shown with plots from a MD simulation of the coalescence of 10 nm diameter Al and Ni nanoparticles. The correlation of the sintering stages to the reaction temperature and time is illustrated in Fig. 8 for the sintering of separate 10 nm diameter nanoparticles. In the initial step the liquid Al nanoparticle, blue atoms in Fig. 6, has melted and is spherical in shape. The solid Ni nanoparticle, red atoms, has large faceted sides and is a single crystal, a typical configuration for a crystalline nanoparticle at low temperatures. During stage 1 the Al nanoparticle is attracted to the Ni surface because of the dual driving forces of surface energy minimization and

FIG. 8. (Color online) Temperature vs time in the sintering of nanoparticles with a Ni:Al ratio of 1:1. The subscripts in the legend refer to the number of atoms of each material and correspond to nanoparticles of diameter of ~3, 5, and 10 nm. The color coded dashed lines are the computed adiabatic temperatures from the thermodynamic analysis. The black dashed line is the predicted temperature for coalescence of bulk Al and Ni.

Ni–Al bond formation. This period lasts about 50 ps in this simulation, as noted in Figs. 6 and 7. Between stages 1 and 2 the driving forces associated with the surface energy are counteracted by a resistance to flow in the Al nanoparticle, causing the coalescence process to slow down dramatically. During stage 2, lasting about 450 ps, the surface area is not changing so that energy release from the surface energy terms has ceased to contribute to the change in system potential energy. The subsequent energy release is entirely attributable to the formation of Ni–Al bonds. This stage lasts a much longer time than the initial nanoparticle coalescence stage and is governed by the material diffusion coefficients. Initially at stage 2 the Ni nanoparticle is still solid and the formation of Ni–Al bonds is only possible by Al diffusing into the Ni core or Ni on the surface of the core melting and diffusing away from the interface. This process proceeds until the Ni core has reached its melting point and mixing of the remaining Ni and Al atoms occurs more rapidly, driven by the enthalpy of formation of NiAl. From stage 2 until complete alloying has occurred, taking ~400 ps, diffusion and mixing of Ni and Al atoms are the primary driving forces.

VI. MD SIMULATION RESULTS OF SEPARATE NANOPARTICLE REACTIVITY

We have previously predicted the adiabatic temperature and sintering time for the reactive sintering process of separate equimolar nanoparticles of Al and Ni. In Fig. 8, the MD simulation results for the equimolar nanoparticles are plotted along with the computed adiabatic temperature for each considered particle size.

From Fig. 8 it is apparent that the predicted adiabatic temperature is in close agreement with the simulated temperature. The variability of the computed temperature arises from the wide range of experimental results for the surface tension for liquid Al and solid Ni, the reported enthalpy of formation for NiAl, and the assumed melting temperature for the Ni and NiAl materials at this scale. Each of these experi-
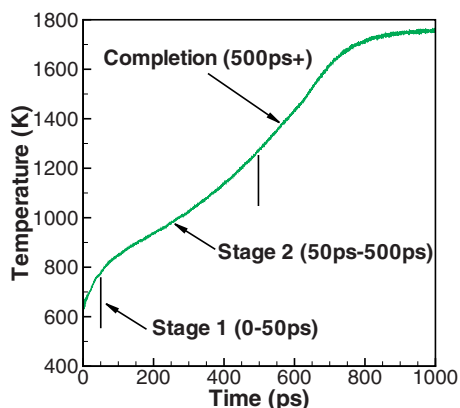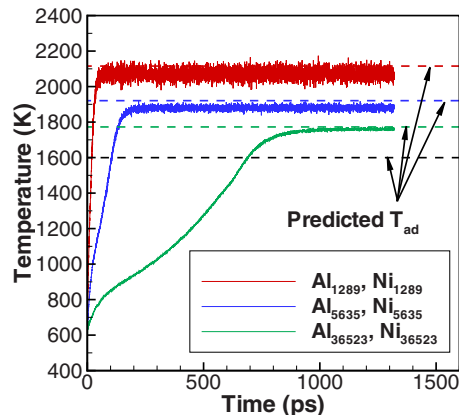

FIG. 7. (Color online) Time vs temperature plot for sintering of separate 10 nm diameter Al and Ni nanoparticles. The various stages of the coalescence processes are denoted on the curve including the final completion stage that occurs after the Ni nanoparticle has melted.
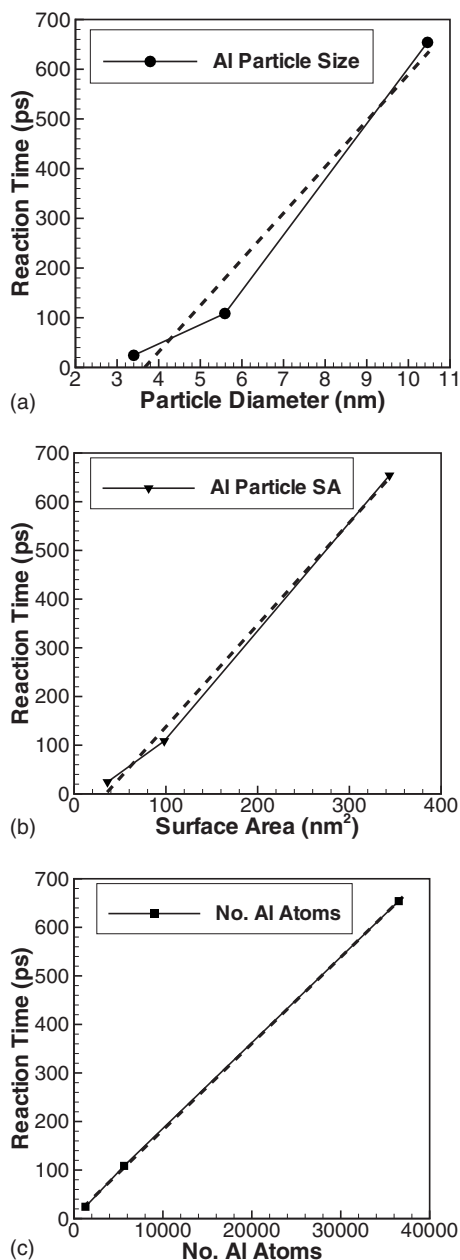
FIG. 9. (a) Reaction time vs Al nanoparticle diameter, (b) Al nanoparticle surface area, and (c) number of Al atoms. Note the nearly linear relationship (dashed line) of reaction time with both the number of atoms (volume) in the Al nanoparticle and the surface area of the Al nanoparticle.

mental data points is used in the thermodynamic analysis and contributes to the small inaccuracies in the predicted temperature.

The characteristic time for reactive synthesis that we use here is defined by Zhao *et al.*[36] as t when

$$T(t) = T_0 + 0.8(T_1 - T_0),\qquad(16)$$

where T_0 is the initial temperature, T_1 is the maximum size dependent temperature reached, and $T(t)$ is the transient temperature. The computed reaction times are given in Fig. 9 and illustrate that the time required for separate nanoparticles to react has a power law relationship that is between nanoparticle volume (c) and surface area (b). This implies that not only will the reaction temperature be higher, but will occur

more rapidly with decreases in particle size, to a power of about 2.5. This is important because a high rate of energy release is desirable for many applications.

By observing the MD simulations and analyzing the shape of the curves in Fig. 8 for temperature versus time we have surmised that there are two reaction rates to consider. The first is during the coalescence process [called the growth rate (see 0–500 ps for Al_{36523} curve in Fig. 8)] and Ni nanoparticle melting and the second is the rapid formation of the NiAl alloy from liquid Al and Ni [convergence rate (see 500 ps and later for the Al_{36523} curve in Fig. 8)]. The temperature at which the transition occurs is size dependent because the melting temperature of the Ni nanoparticle is also size dependent. If the process is not perfectly adiabatic and some heat is lost to the surroundings, it is also possible that the first process would not precede far enough for the Ni nanoparticle to melt and thus the reaction would halt. This would only occur with larger nanoparticles that require longer reaction times during which some energy loss to the surroundings is likely. This is an important consideration in real world applications that are not perfectly adiabatic, but when complete alloying is desired. One reason for this observed increase in reaction rate is because the heat generated from the formation of Ni–Al bonds will conduct into the core nanoparticle so that when the reaction front reaches the inner atoms they will have a higher diffusion coefficient, which in turn increases the reaction rate.

VII. REACTIVE SINTERING OF CORE-SHELL NANOPARTICLES

A. Aluminum coated nickel

In this section we will discuss the sintering process for an Al-coated Ni nanoparticle followed by a discussion of a Ni-coated Al nanoparticle. Both of these systems can be used as a model for highly compacted Ni and Al nanoparticles or one material serving as a matrix for nanoparticles of the other. In the first model system we assume that a Ni nanoparticle has been coated with Al and equilibrated without the Ni melting or any further reaction occurring. The results for the reaction time and temperature will be presented and a comparison with the separate nanoparticle case will be given. Here again we have considered three system sizes with 1289, 5635, and 36523 atoms each of Al and Ni.

An initial estimate is that the coalescence process for the fully coated nanoparticle system will be a truncated version of the separate nanoparticle case. In the coated nanoparticle system we do not have the first stage of coalescence occurring and only observe the second stage, namely, diffusion of Ni and Al atoms to form Ni–Al bonds. The sintering temperature versus time plot is given in Fig. 10 and shows an interesting result. Whereas the maximum temperature reached increases with decreasing nanoparticle size for coalescence of separate nanoparticles, the opposite is true here. The temperature decreases with decreasing nanoparticle size.

In Fig. 10 the observed decrease in adiabatic temperature is due to the fact that the ratio of atoms near the interfacial region to the atoms in the bulk nanoparticle decreases as the nanoparticle size increases. Atoms in the interfacial region
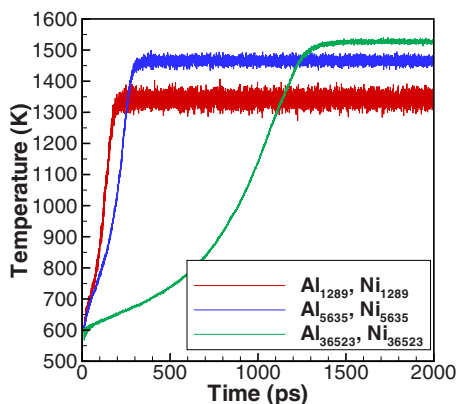
FIG. 10. (Color online) Temperature vs time in the sintering of Al-coated Ni nanoparticles with a Ni:Al ratio of 1:1.

FIG. 12. Reaction time vs number of Al atoms in the Al-coated Ni nanoparticle system.

have already formed Ni–Al bonds and are therefore already at a lower configurational energy than if they were contained in a homogeneous nanoparticle of either pure Al or Ni. If we extend the adiabatic temperature relationship to infinitely large particles we would approach the result obtained from the analysis of separate nanoparticle as they increase in size. The thermodynamic analysis is similar except that the surface energy term is zero and the enthalpy of formation is lowered by a factor proportional to the ratio of surface area to volume. The enthalpy of the products [Eq. (5)] modified for coated nanoparticles becomes

$$H_{prod} = \left(1 - \frac{tA_{surface}}{V}\right)H_{form,NiAl} + \int_{298\ K}^{T_{ad}} C_{p,NiAl}(T)dT$$
$$+ H_{melt,Ni}, \tag{17}$$

where t is a computed thickness value for the interfacial layer, $A_{surface}$ is the area of the interfacial region, and V is the volume of the Ni core. In order to determine the correct empirical thickness value t for Eq. (17) we have used the adiabatic temperature computed in the MD simulation results for the Al-coated Ni nanoparticle. These results indicate that an interface thickness of 0.07 nm is able to accurately predict the adiabatic temperature observed in the MD simulations (Fig. 11). In Fig. 11 it is apparent that the adiabatic combustion temperature is highly size dependent for nanoparticles of less than 10 nm in diameter. For very small nanoparticles of
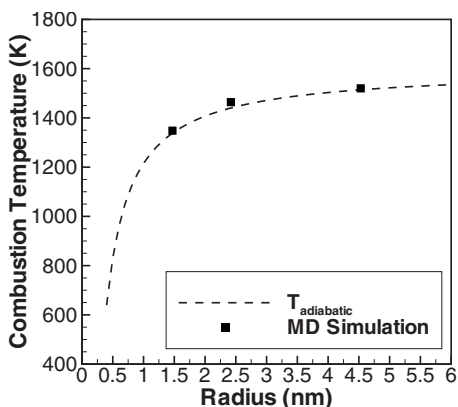
less than 1 nm diameter, there is a little predicted change in temperature from the initial temperature of 600 K since most of the potential Ni–Al bonds have already been formed.

From the sintering of separate nanoparticles it is expected that the reaction time will be linearly related to the radius of the nanoparticle to a power of about 2.5. In Fig. 12 this appears to be the case for this range of nanoparticle sizes. A slight deviation from the separate nanoparticle result is probably related to the fact that the coalescence process, stage 1, is not included in this model system and diffusion takes longer to initialize the energetic reaction process.

The results for the Al-coated Ni nanoparticle indicate the trends that one might expect from a material system that included an Al matrix with embedded Ni nanoparticles. From the results in Figs. 11 and 12 there are two competing reaction results, namely, reaction time and maximum temperature. In Fig. 12 we see that as the Ni nanoparticle size decreases the reaction time decreases, causing the energy release rate to increase. A second observation that can be made from Fig. 11 is that the reaction temperature decreases with decreasing Ni nanoparticle size, potentially minimizing the effect of the rapid energy release.

Looking more closely at the reaction time versus number of atoms for the separate nanoparticle and Al-coated Ni nanoparticle cases, we observe a similar relationship of reaction time to nanoparticle size as that found in separate nanoparticles. In both cases the reaction time appears to have a power law relationship with radius with an exponent of 2.5. The accelerated temperature increase in Fig. 10 after about 900 ps for the Al_{36523} curve is the convergence rate discussed previously.

B. Nickel coated aluminum

The Ni-coated Al nanoparticle system has garnered some interest because when Al melts there is an experimentally observed increase in volume of about 6.5%. This increase in volume creates a large stress in the Ni coating and may result in catastrophic failure and fragmentation of the nanoparticle.[18] In the work of Delogu,[18] the fragmentation is only observed for a specific set of conditions including Ni shell thickness. In this work, even with the appropriate Ni shell thickness, the fragmentation of the nanoparticle is not

FIG. 11. Comparison of thermodynamically determined adiabatic temperature for Al-coated Ni nanoparticle and results from MD simulation.
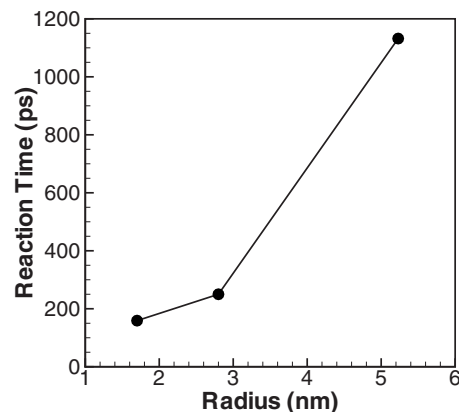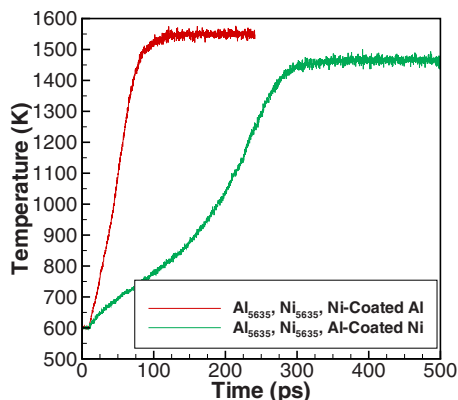
FIG. 13. (Color online) Comparison of combustion temperature for Ni-coated Al nanoparticle vs Al-coated Ni nanoparticle.

observed. With the empirical potentials and parameters considered here the energetic alloying reaction is fast and results in a liquid NiAl nanoparticle without fragmentation.

In the first set of analyses the Ni shell contains the same number of atoms as the Al core. This results in an Al core with a radius of 2.8 nm and a Ni shell of about 0.7 nm. Since the bond length of Ni is less than Al the shell is thinner and the contact area is initially greater than that observed in similarly sized Al-coated Ni nanoparticles. As with the nanoparticle coalescence simulations, the temperature of the system is raised to 600 K at which time a constant energy simulation is used to analyze the energy conversion rate and the adiabatic temperature rise in the system.

In the initial simulations with an atomic ratio of unity there are more Ni–Al bonds in the Ni-coated nanoparticle than the Al-coated nanoparticle. It may therefore be expected that the total system energy would initially be lower in the Ni-coated Al nanoparticle system than the Al-coated Ni system. In fact, the opposite is true because although there are more Ni–Al bonds in the Ni-coated system there are fewer Ni–Ni bonds than in the Al-coated nanoparticle. Since Ni–Ni bonds are stronger than Al–Al bonds the total initial energy is lower in the Al-coated Ni nanoparticle system. Since the final configuration of both systems is a completely alloyed NiAl nanoparticle, the system energy change for the Ni-coated nanoparticle is greater than the Al-coated system. This greater change in potential energy results in the computed adiabatic temperature for the Ni-coated Al nanoparticle being higher than the Al-coated nanoparticle (Fig. 13) although the difference is not large.

In the two following simulations we simulated an ~5 nm diameter Al nanoparticle coated with either a 1 or 2 nm thick Ni coating (Fig. 14). For these simulations the temperature was controlled using a canonical ensemble average or NVT ensemble average. This temperature control was used in order to rapidly increase the temperature from about 300 K to above the melting point of the Al nanoparticle at a rate of 0.1 K/ps. When the Al nanoparticle melts and expands, a large sudden increase in stress in the Ni coating is observed. For the 2 nm thick Ni coating the increase in stress is not high enough to cause failure of the coating. In this case the outer shell expands slightly but does not crack. For the 1 nm thick case the stress in the Ni shell is high enough to
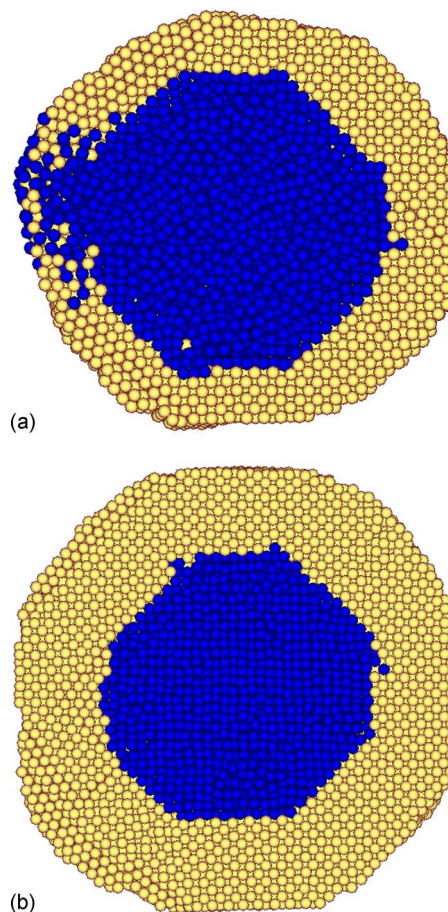

FIG. 14. (Color online) Cross sections of the Ni-coated Al nanoparticle simulation model just after melting of the Al core for (a) 1 nm and (b) 2 nm thick Ni shells.

cause failure. When the shell fails the Al begins to leak out onto the surface of the nanoparticle but no fragmentation is observed. If the nanoparticle was surrounded by oxygen this may initiate the Al oxidation reaction, releasing additional energy as Al oxides are formed.

The cracking and leaking of Al onto the surface of the Ni shell are very different from what Delogu[18] observed using a semi-empirical tight-binding potential. Another difference from the work of Delogu is the choice of Al core radius. For both of the shell cases here the core has a radius of 2.8 nm. This is in contrast to the core radius of 3.0 and 2.0 nm for the 1.0 and 2.0 nm shell cases, respectively, used by Delogu.[18] Since the 1 nm shell case is the most interesting and the radii are very close (2.8 nm versus 3.0 nm) the choice of core size is not expected to have had an appreciable effect on the results for this case.

Throughout this simulation effort, oxygen in the form of free molecules or metal oxides is not considered. This is primarily due to the fact that including oxygen in the simulations would require computing charge transfer[37,38] which would limit the size and scope of the model configurations considered. From the knowledge on the binding energy for Al and Ni oxides it is possible to estimate what effect an oxide coating will have on the various configurations considered here. For the sintering of separate particles an oxide coating would act as a passivating layer because of the high

melting points of these oxides, 2327 K for Al_2O_3 and 2257 K for NiO. This passivation layer will likely need to be removed by mechanical failure or melting before complete sintering could take place, increasing the temperature required for activation of the sintering process. A similar effect will likely be observed in the coated nanoparticle models if an oxide layer is present between the two metals. For free oxygen molecules surrounding sintering nanoparticles the oxidation reaction would take precedence over the SHS reaction where competition exists on exposed surfaces because of the much higher enthalpies of formation for the oxides over the formation of Ni–Al bonds.

VIII. CONCLUSIONS

We have analyzed two model systems for the energetic reaction of Ni and Al. In the first case we considered the coalescing and sintering of separate nanoparticles and found that the energy release from the change in surface area is only significant with small, less than 10 nm diameter nanoparticles. These separated nanoparticle reaction simulations and thermodynamic analyses show that the reaction time will decrease and the adiabatic reaction temperature will increase with decreasing nanoparticle sizes. This may be important for applications where high energy release rates are desired. The simulation data closely match a classical thermodynamic analysis.

In the second part of this work we considered the sintering of Al-coated Ni nanoparticles and Ni-coated Al nanoparticles as a model material system for nanoparticles embedded in a matrix of the other metal. This work revealed that the reaction time is again inversely related to nanoparticle size but the adiabatic temperature decreases with decreasing nanoparticle size. Mechanically the Al-coated Ni nanoparticle system is a model system for a lightweight Al matrix with embedded Ni nanoparticles, a system with a relatively high strength compared to a loosely bonded powder of Al and Ni nanoparticles. This Al matrix system could be used in systems where mechanical strength is important in addition to energy release from kinetic sintering of the Ni and Al atoms. In the Ni-coated Al nanoparticle system we investigated possible rupture and fragmentation of the Ni shell but were unable to observe any fragmentation.

ACKNOWLEDGMENTS

[1] X. Phung, J. Groza, E. A. Stach, L. N. Williams, and S. B. Ritchey, Mater. Sci. Eng., A **359**, 261 (2003).
[2] A. Rai, D. Lee, K. Park, and M. R. Zachariah, J. Phys. Chem. B **108**, 14793 (2004).
[3] H. P. Li, Mater. Sci. Eng., A **404**, 146 (2005).
[4] S. Gennari, U. A. Tamburini, F. Maglia, G. Spinolo, and Z. A. Munir, Acta Mater. **54**, 2343 (2006).
[5] P. Nash and O. Kleppa, J. Alloys Compd. **321**, 228 (2001).
[6] R. Hu and P. Nash, J. Mater. Sci. **40**, 1067 (2005).
[7] J. C. Trenkle, T. P. Weihs, and T. C. Hufnagel, Scr. Mater. **58**, 315 (2008).
[8] S. Dong, P. Hou, H. Cheng, H. Yang, and G. Zou, J. Phys.: Condens. Matter **14**, 11023 (2002).
[9] L. J. Lewis, P. Jensen, and J.-L. Barrat, Phys. Rev. B **56**, 2248 (1997).
[10] T. Hawa and M. R. Zachariah, Phys. Rev. B **71**, 165434 (2005).
[11] T. Hawa and M. R. Zachariah, J. Aerosol Sci. **37**, 1 (2006).
[12] M. R. Zachariah and M. J. Carrier, J. Aerosol Sci. **30**, 1139 (1999).
[13] S. H. Ehrman, J. Colloid Interface Sci. **213**, 258 (1999).
[14] S. Arcidiacono, N. R. Bieri, D. Poulikakos, and C. P. Grigoropoulos, Int. J. Multiphase Flow **30**, 979 (2004).
[15] S. Yu, C.-Y. Wang, T. Yu, and J. Cai, Physica B **396**, 138 (2007).
[16] Y. Mishin, M. J. Mehl, and D. A. Papaconstantopoulos, Phys. Rev. B **65**, 224114 (2002).
[17] J. Mei, B. R. Cooper, and S. P. Lim, Phys. Rev. B **54**, 178 (1996).
[18] F. Delogu, Nanotechnology **18**, 505702 (2007).
[19] H. X. Zhu and R. Abbaschian, J. Mater. Sci. **38**, 3861 (2003).
[20] S. J. Plimpton, J. Comput. Phys. **117**, 1 (1995).
[21] M. W. Finnis and J. E. Sinclair, Philos. Mag. A **50**, 45 (1984).
[22] J. E. Angelo, N. R. Moody, and M. I. Baskes, Modell. Simul. Mater. Sci. Eng. **3**, 289 (1995).
[23] G. J. Ackland and V. Vitek, Phys. Rev. B **41**, 10324 (1990).
[24] P. Pawlow, Z. Phys. Chem. **65**, 545 (1909).
[25] P. Zhu, J. C. M. Li, and C. T. Liu, Mater. Sci. Eng., A **357**, 248 (2003).
[26] R. Arroyave, D. Shin, and Z.-K. Liu, Acta Mater. **53**, 1809 (2005).
[27] F. Z. Chrifi-Alaoui, M. Nassik, K. Mahdouk, and J. C. Gachon, J. Alloys Compd. **364**, 121 (2004).
[28] M. R. Zachariah, M. J. Carrier, and E. Blasiten-Barojas, J. Phys. Chem. **100**, 14856 (1996).
[29] M. P. Allen and D. J. Tildesley, *Computer Simulation of Liquids* (Clarendon, Oxford, 1996).
[30] V. I. Nizhenko, Powder Metall. Met. Ceram. **43**, 273 (2004).
[31] A. Y. Lozovoi, A. Alavi, and M. W. Finnis, Phys. Rev. Lett. **85**, 610 (2000).
[32] O. Kubaschewski, *Materials Thermochemistry*, 6th ed., Pergamon Press, New York, 1993, p. 299.
[33] D. Mukherjee, C. G. Sonwane, and M. R. Zachariah, J. Chem. Phys. **119**, 3391 (2003).
[34] J. Frenkel, J. Phys. (Moscow) **9**, 385 (1945).
[35] M. A. Assael, K. Kakosimos, R. M. Banish, J. Brillo, I. Egry, R. Brooks, P. N. Quested, K. C. Mills, A. Nagashima, Y. Sato, and W. A. Wakeham, J. Phys. Chem. Ref. Data **35**, 285 (2006).
[36] S. Zhao, T. C. Germann, and A. Strachan, J. Chem. Phys. **125**, 164707 (2006).
[37] Q. Zhang, T. Çağın, A. van Duin, W. A. Goddard III, Y. Qi, and L. G. Hector, Jr., Phys. Rev. B **69**, 045423 (2004).
[38] F. H. Streitz and J. W. Mintmire, Phys. Rev. B **50**, 11996 (1994).